

Supporting Information

Mitochondria-targeting cyclometalated iridium(III) complexes for tumor hypoxic imaging and therapy

Jia Li,^a Hongmin Chen,^a Leli Zeng,^a Thomas W. Rees,^a

Kai Xiong,^a Yu Chen,^{*a} Liangnian Ji,^a Hui Chao^{*a,b}

^a MOE Key Laboratory of Bioinorganic and Synthetic Chemistry, School of Chemistry, Sun Yat-Sen University, Guangzhou 510275, P. R. China

^b MOE Key Laboratory of Theoretical Organic Chemistry and Functional Molecule, School of Chemistry and Chemical Engineering, Hunan University of Science and Technology, Xiangtan, 400201, P. R. China

E-mail: ceschh@mail.sysu.edu.cn; chenyu63@mail.sysu.edu.cn

Contents

Experimental Section.....	S4
Materials.....	S4
Synthesis and characterization.....	S4
Scheme S1 Synthetic routes of ligands and Ir(III) complexes.....	S8
Octanol/water partition coefficients (Log <i>P</i>) measurement.....	S9
Cell lines and culture conditions.....	S9
Preparation of fresh rat liver microsomes.....	S9
<i>In Vitro</i> Cytotoxicity.....	S10
3D multicellular spheroid formation.....	S10
Real-time cell growth and proliferation assay.....	S11
Cellular entry mechanism studies.....	S11
Intracellular localization studies.....	S12
Live/dead viability/cytotoxicity assay in the MCTSs.....	S12
Acridine orange/ethidium bromide (AO/EB) staining.....	S13
Induction of mitochondrial dysfunction.....	S13
Caspase-3 activation detection.....	S13
Western blot analysis.....	S14
Real-time monitoring of hypoxic cell assay.....	S14
Figure S1 ESI-MS spectrum of L3	S15
Figure S2 ¹ H NMR spectrum of L3	S15
Figure S3 ESI-MS spectrum of L4	S16
Figure S4 ¹ H NMR spectrum of L4	S16
Figure S5 ESI-MS spectrum of L5	S17
Figure S6 ¹ H NMR spectrum of L5	S17
Figure S7 ESI-MS spectrum of Ir1	S18
Figure S8 ¹ H NMR spectrum of Ir1	S18
Figure S9 ESI-MS spectrum of Ir2	S19
Figure S10 ¹ H NMR spectrum of Ir2	S19

Figure S11 ESI-MS spectrum of Ir3	S20
Figure S12 ¹ H NMR spectrum of Ir3	S20
Figure S13 ESI-MS spectrum of Ir4	S21
Figure S14 ¹ H NMR spectrum of Ir4	S21
Figure S15 ESI-MS spectrum of Ir5	S22
Figure S16 ¹ H NMR spectrum of Ir5	S22
Figure S17 HPLC spectrum of Ir1-5	S23
Figure S18 Stability in Human Plasma.....	S23
Figure S19 Hypoxia response study of Ir1	S24
Figure S20 Hypoxia response study of Ir3	S25
Figure S21 Hypoxia response study of Ir4	S26
Figure S22 Hypoxia response study of Ir5	S27
Figure S23 Selective recognition study.....	S28
Figure S24 Octanol/water partition coefficients measurement.....	S29
Figure S25 Kinetics of cytotoxicity.....	S30
Figure S26 the mechanism of intercellular uptake.....	S31
Figure S27 Western blot analysis.....	S31
References.....	S31

Experimental Section:

Materials

All of the reagents were purchased from commercial sources and used without further purification, unless stated otherwise. All of the buffer components were of biological grade. IrCl₃, ppy, phen, Cisplatin, JC-1, dimethyl sulfoxide (DMSO) and 3-(4,5-dimethylthiazol-2-yl)-2,5-diphenyltetrazolium bromide (**MTT**) were purchased from Sigma Aldrich. Nucleoprotein Extraction Kit and Cytoplasmic and Mitochondrial Protein Extraction Kit (Sangon Biotech) All the compounds tested were dissolved in DMSO just before the experiments and the final DMSO concentration was less than 1% (v/v). The Electrospray ionization mass spectra (ESI-MS) were recorded on a LCQ system (Finnigan MAT, USA). Microanalysis (C, H, and N) was carried out by using an Elemental Vario EL CHNS analyzer (Germany). The ¹H NMR spectra were recorded on a Mercury-Plus 300 spectrometer (300 MHz). All of the chemical shifts are reported relative to tetramethylsilane (TMS). The filtrate was analyzed by HPLC spectroscope (Thermo, USA). Electronic absorption spectra were recorded using a Perkin-Elmer Lambda850 UV/Vis spectrometer. Emission spectra were recorded on a Perkin-Elmer LS 55 luminescence spectrometer.

Synthesis and characterization

Synthesis of the Ligands: **L1** and **L2** prepared as previously reported by our group.¹ **L3-5** were prepared as follows: A mixture of 1,10-phenanthroline-5,6-dione (212 mg, 1 mmol), 2-formyl-9,10-anthraquinone (236 mg, 1.0 mmol), the relevant aniline (1.2 mmol), ammonium acetate (949 mg, 12.23 mmol), and glacial acetic acid (10 mL) was refluxed under argon for 24 h. After the reaction mixture was cooled to room temperature the solution was neutralized with 25% NH₃ aqueous solution. The resulting precipitate was collected by vacuum filtration. The crude product was purified by column chromatography on silica with a CH₂Cl₂-EtOH mix as the eluent.

Synthesis and Characterization of L3: This ligand was synthesized in a similar manner to that described for the **L1**, except that 4-Fluoroaniline (133 mg, 1.2 mmol) was used instead of p-aminotoluene. Yield 221.1 mg, 42.5%. Calculated for ESI-MS: 521.14 and obtained (CH₂Cl₂/CH₃OH 1:1) $m/z = 521.61$ [M+H]⁺. Elemental analysis: calcd(%) for C₃₃H₁₇FN₄O₂: C 76.15, H 3.29, N 10.76, found: C 76.31, H 3.53, N 10.59. ¹H NMR (400 MHz, CDCl₃) δ 9.44 (d, $J = 8.2$ Hz, 1H), 9.12 (s, 1H), 8.92 (s, 1H), 8.19 (s, 1H), 8.12 – 8.06 (m, 1H), 8.01 – 7.95 (m, 3H), 7.85 – 7.81 (m, 1H), 7.57 – 7.54 (m, 2H), 7.50 (dd, $J = 8.2, 2.9$ Hz, 2H), 7.45 – 7.41 (m, 2H), 7.22 (d, $J = 8.2$ Hz, 2H).

Synthesis and Characterization of L4: This ligand was synthesized in a similar manner to that described for the **L1**, except that p-anisidine (148 mg, 1.2 mmol) was used instead of p-aminotoluene. Yield 268.94 mg, 45.2%. Calculated for ESI-MS: 533.16 and obtained (CH₂Cl₂/CH₃OH 1:1) $m/z = 533.58$ [M+H]⁺. Elemental analysis: calcd(%) for C₃₄H₂₀N₄O₃: C 76.68, H 3.79, N 10.52, found: C 76.53, H 3.93, N 10.37. ¹H NMR (400 MHz, CDCl₃) δ 9.46 (s, 1H), 9.36 (d, $J = 8.0$ Hz, 1H), 9.23 (d, $J = 4.0$ Hz, 1H), 8.59 (s, 1H), 8.29 (t, $J = 6.1$ Hz, 4H), 8.11 (d, $J = 8.2$ Hz, 1H), 7.99 (dd, $J = 7.7, 4.8$ Hz, 1H), 7.90 – 7.79 (m, 3H), 7.65 (d, $J = 8.4$ Hz, 1H), 7.56 (d, $J = 8.7$ Hz, 3H), 7.51 – 7.47 (m, 1H), 7.25 (d, $J = 8.8$ Hz, 2H).

Synthesis and Characterization of L5: This ligand was synthesized in a similar manner to that described for the **L1**, except that 4-Phenoxyaniline (222 mg, 1.2 mmol) was used instead of p-aminotoluene. Yield 248.9 mg, 46.7%. Calculated for ESI-MS: 595.18 and obtained (CH₂Cl₂/CH₃OH 1:1) $m/z = 595.74$ [M+H]⁺ Elemental analysis: calcd(%) for C₃₉H₂₂N₄O₃: C 78.78, H 3.73, N 9.42, found: C 78.61, H 3.99, N 9.27. ¹H NMR (400 MHz, CDCl₃) δ 9.31 (d, $J = 3.1$ Hz, 1H), 9.24 (d, $J = 8.0$ Hz, 1H), 9.17 (d, $J = 3.1$ Hz, 1H), 8.42 – 8.31 (m, 5H), 7.89 – 7.82 (m, 3H), 7.73 (d, $J = 7.2$ Hz, 1H), 7.60 (d, $J = 8.7$ Hz, 2H), 7.50 – 7.45 (m, 2H), 7.36 (d, $J = 8.7$ Hz, 2H), 7.32 (s, 3H), 7.26 (d, $J = 7.4$ Hz, 1H).

Synthesis and Characterization of Ir1: [Ir(ppy)₂Cl]₂ (53.8 mg, 0.05 mmol) and the **L1** (51.6 mg, 0.1 mmol) in CHCl₃/CH₃OH (10 mL/8 mL) was refluxed under an argon

atmosphere at 65 °C for 8 hours, the solution was cooled to room temperature then evaporated to dryness after the reaction. The product obtained were purified by column chromatography on alumina with CH₂Cl₂/EtOH. Yield 45.4 mg, 43.1%. Calculated for ESI-MS:1017.25 and obtained (CH₃OH) $m/z = 1017.50 [M]^+$. Elemental analysis: calcd(%) for C₅₆H₃₆ClIrN₆O₂: C 63.90, H 3.45, N 7.99, found: C 63.77, H 3.61, N 7.83. ¹H NMR (300 MHz, DMSO-d₆) δ 9.34 (d, $J = 8.2$ Hz, 1H), 8.60 (s, 1H), 8.44 (d, $J = 5.9$ Hz, 1H), 8.37–8.12 (m, 7H), 8.05 (s, 1H), 8.01–7.89 (m, 7H), 7.80–7.56 (m, 7H), 7.21 (dd, $J = 15.5, 7.8$ Hz, 2H), 7.10 (t, $J = 7.2$ Hz, 2H), 7.02 (t, $J = 7.0$ Hz, 2H), 6.50 (t, $J = 7.1$ Hz, 2H), 2.68 (s, 3H). Purity: 97.47%

Synthesis and Characterization of Ir2: This complex was synthesized in a similar manner to that described for the **Ir1**, except that **L2** (55.8 mg, 0.1 mmol) was used instead of **L1**. Yield 42.7 mg, 39.0%. Calculated for ESI-MS: 1059.30 and obtained (CH₃OH) $m/z = 1059.60 [M]^+$. Elemental analysis: calcd(%) for C₅₉H₄₂ClIrN₆O₂: C 64.72, H 3.87, N 7.68, found: C 64.59, H 4.02, N 7.60. ¹H NMR (300 MHz, DMSO-d₆) δ 9.36 (d, $J = 7.8$ Hz, 1H), 8.25–8.10 (m, 10H), 7.91 (s, 6H), 7.78 (s, 5H), 7.63 (d, $J = 7.5$ Hz, 1H), 7.49 (s, 2H), 6.98 (d, $J = 25.2$ Hz, 6H), 6.26 (s, 2H), 1.41 (s, 9H). Purity: 98.84%

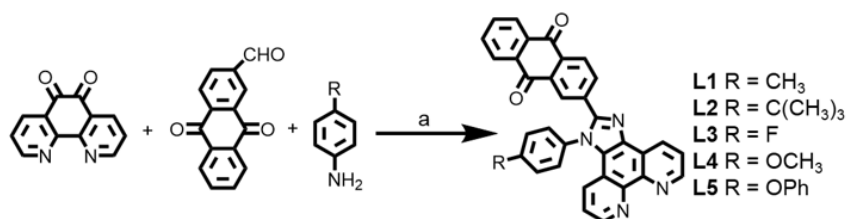
Synthesis and Characterization of Ir3: This complex was synthesized in a similar manner to that described for the **Ir1**, except that **L3** (52.0 mg, 0.1 mmol) was used instead of **L1**. Yield 34.2 mg, 32.4%. Calculated for ESI-MS: 1021.23 and obtained (CH₃OH) $m/z = 1021.30 [M]^+$. Elemental analysis: calcd(%) for C₅₅H₃₃ClIrN₆O₂: C 62.51, H 3.15, N 7.96, found: C 62.39, H 3.30, N 7.82. ¹H NMR (300 MHz, DMSO-d₆) δ 9.37 (d, $J = 8.1$ Hz, 1H), 8.35 (s, 1H), 8.30–8.10 (m, 9H), 8.01–7.81 (m, 9H), 7.64 (d, $J = 7.9$ Hz, 3H), 7.48 (s, 2H), 7.10–6.89 (m, 6H), 6.27 (t, $J = 8.4$ Hz, 2H). Purity: 98.54%

Synthesis and Characterization of Ir4: This complex was synthesized in a similar manner to that described for the **Ir1**, except that **L4** (53.2 mg, 0.1 mmol) was used instead of **L1**. Yield 47.5 mg, 44.5%. Calculated for ESI-MS: 1033.25 and obtained

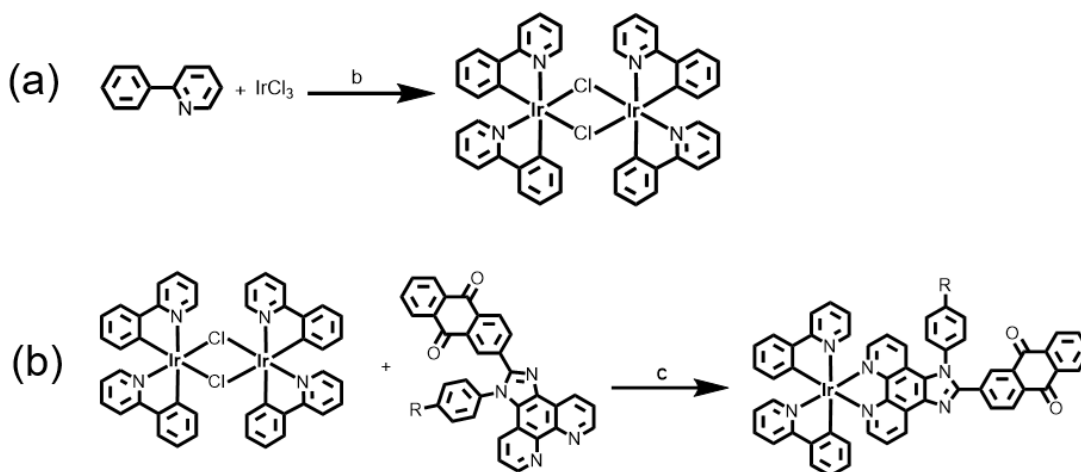
(CH₃OH) $m/z = 1033.20$ [M]⁺ Elemental analysis: calcd(%) for C₅₆H₃₆ClIrN₆O₃: C 62.93, H 3.39, N 7.86, found: C 62.81, H 3.61, N 7.76. ¹H NMR (300 MHz, DMSO-d₆) δ 9.36 (d, $J = 7.7$ Hz, 1H), 8.46 (s, 1H), 8.30–8.07 (m, 9H), 7.99–7.76 (m, 9H), 7.62 (d, $J = 8.4$ Hz, 1H), 7.48 (s, 2H), 7.28 (s, 2H), 7.09–6.89 (m, 6H), 6.26 (t, $J = 8.2$ Hz, 2H), 3.90 (s, 3H). Purity: 95.65%

Synthesis and Characterization of Ir5: This complex was synthesized in a similar manner to that described for the **Ir1**, except that **L5** (59.4 mg, 0.1 mmol) was used instead of **L1**. Yield 57.8 mg, 51.2%. Calculated for ESI-MS: 1095.26 and obtained (CH₃OH) $m/z = 1095.20$ [M]⁺. Elemental analysis: calcd(%) for C₆₁H₃₈ClIrN₆O₃: C 64.79, H 3.39, N 7.43, found: C 64.62, H 3.72, N 7.32. ¹H NMR (300 MHz, DMSO-d₆) δ 9.37 (d, $J = 8.5$ Hz, 1H), 8.40–8.08 (m, 10H), 8.00–7.82 (m, 9H), 7.77 (d, $J = 7.6$ Hz, 1H), 7.46 (d, $J = 14.5$ Hz, 4H), 7.38 (d, $J = 7.0$ Hz, 2H), 7.30–7.17 (m, 3H), 7.11–6.89 (m, 6H), 6.26 (t, $J = 8.2$ Hz, 2H). Purity: 96.19%

Ligands Synthesis



Ir(III) Complexes Synthesis:



Ir1 R = CH₃; Ir2 R = C(CH₃)₃; Ir3 R = F; Ir4 R = OCH₃; Ir5 R = OPh

Scheme S1 Synthetic routes of ligands and Ir(III) complexes: Reaction conditions: (a) NH₄Ac, HAc, 120 °C reflux, 24 h, Ar. yield: **L1**, 42.5%, **L2**, 44.5%, **L3**, 42.5%, **L4**, 45.2%, **L5**, 46.7. (b) 2-ethoxyethanol/H₂O, 100 °C, 24 h, Ar. (c) methanol/CHCl₃, 65 °C, 8 h, Ar. yield: **Ir1**, 43.1%, **Ir2**, 42.7%, **Ir3**, 32.4%, **Ir4**, 44.5%, **Ir5**, 51.2%.

Octanol/water partition coefficients (Log $P_{o/w}$) measurement

The partition-coefficient of each complex be determined by "shake-flask" method.² Water and octanol were mixed for 12 h to full saturation and two layers were separated. The complexes were dissolved in the octanol phase which was previously saturated with water to give a 5 mL solution. The same volume of water phase previously saturated with octanol was added into the solution. The mixture was shaken vigorously at room temperature for 12 hours. The concentration of **Ir1-5** was measured by UV-vis spectroscopy. The evaluation was carried out in triplicate. The Log $P_{o/w}$ value was calculated according to formula below:

$$\text{Log } P_{o/w} = \log \left(\frac{[\text{solute}]_{\text{octanol}}}{[\text{solute}]_{\text{water}}} \right)$$

Cell lines and culture conditions

Human cervical carcinoma cell line (HeLa), lung carcinoma cell lines (A549R A549), Human hepatoma cell line (HepG2), human hepatocyte cell line (LO2) were obtained from the ATCC and were cultured in DMEM with 37 °C and 5% CO₂ supplemented with 10% inactivated fetal bovine serum (FBS) and 1% penicillin-streptomycin (Gibco, USA). The hypoxic culture conditions are similar to the normoxic conditions, with 1 % O₂ in place of 20% O₂, the concentration of oxygen is controled by ventilation with high-purity nitrogen gas in an incubator.

Preparation of fresh rat liver microsomes

Rats (Wistar, 7 weeks) fasted overnight and intraperitoneal injected 80 mg/kg pentobarbitalsodium. The liver placed in 0.15 M KCl solution (pH 7.4) and homogenized in three volumes of the same buffer. Hypoxic condition was generated by bubbling argon gas into the reaction solution for 30 minutes. Rat liver microsomes (0.25 mg protein/mL) and 50μM NADPH were pre-incubated at 37 °C for 30 min. phosphorescence probe (2.5μM) containing 0.1% DMSO was added as a co-solvent.

The *in vitro* enzyme assay was extracted with chloroform and analyzed by ESI-MS in mixture solution.

In Vitro Cytotoxicity

Seeded cell monolayer in triplicate into 96-well plates at a density of 1×10^4 cells/well with supplemented culture medium (100 μ L/well) and incubated in standard culturing condition (5% CO₂, 10% FBS, 1% penicillin-streptomycin at 37 °C) for 24 h. Then the complex was incubated Hella cell for 44 hours. After that, cytotoxicity was evaluated by the MTT assay; 20 μ L of MTT solution (5 mg/mL in $1 \times$ PBS) was added to each well and then placed at 37 °C for 4 h. All solution was gently removed and DMSO (150 μ L) was added to each well, the optical density of each well was measured by a microplate spectrophotometer (Biorad, USA) at 595 nm.

3D multicellular spheroid formation

The cytotoxicities of the complexes towards 3D multicellular spheroids were evaluated by a cell spheroid growth inhibition assay. Hella cell 150 μ L of a 2.5×10^4 cells/mL single cell suspension was plated onto agarose-coated (sterile, 1% (w/v) in PBS, 50 μ L) 96-well imaging plates, the allowed to aggregate for 96 h without motion until the balls of cells were formed. The spheroids 500-600 μ m in diameter were incubated with **Ir1-5** (2.0 μ M) for 6 h, then Confocal laser scanning microscopy was used to image the spheroids. The small cell spheroids 100-150 μ m in diameter were formed by the addition 150 μ L of a 2.5×10^3 cells/mL single cell suspension that was allowed to aggregate for 48 h. These were then incubated with **Ir1-5** (2.0 μ M). The spheroids were measured and imaged with an inverted fluorescence microscope (Zeiss) every 24 h for 7 days.

Real-time cell growth and proliferation assay

Real-time cell growth and proliferation assay was carried out by using an xCELLigence RTCA DP system real-time cell analyzer (Roche Diagnostics GmbH, Germany), which was placed in a humidified incubator maintained with 5% CO₂ and 1 % O₂ at 37 °C. Growth curves were obtained by using 16-well plates (E-plate 16, Roche Diagnostics GmbH, Germany). The theory here is that the cell status based on the measured cell electrode impedance, the parameter cell index (CI) is a relative value to indicate the number of cells on the electrodes and the slope of the CI curve reflects the growth speed of the cells. The E-plate 16 was connected to the system and the cell culture medium (50 µL) was added into each well. In order to check the electrical contacts are good, the background impedance was also automatically measured after 30 s. Then, Hella cells 100 µL of a 5×10^4 cells/mL single cell suspension were added onto the wells of the E-plate 16. About 24 h after seeding, **Ir1-5** (0.5, 1, 2.0, or 4.0 µm) were added and the cells were automatically monitored over 75 h by the xCELLigence system. Data was analyzed using the RTCA software.

Cellular entry mechanism studies

HeLa cells were seeded on 35 mm confocal dishes at a density of 1×10^4 cells/mL and cultured overnight. For metabolic inhibition, the cells were incubated with **Ir2** (2 µM) for 1 h at 4 °C or pretreated with 2- deoxy-d-glucose (50 mM) and oligomycin (5 µM) in PBS for 1 h at 37 °C and then incubated with of **Ir2** (2 µM) at 37 °C for another 1 h. For endocytic inhibition, the cells were pre-incubated with NH₄Cl (50 mM) or chloroquine (100 µM) in PBS for 1 h at 37 °C and then incubated with **Ir2** (2 µM) for another 1 h. The medium was removed and washed with PBS for three times and then imaged by using confocal microscope.

Intracellular localization studies

The intracellular localization studies of the complexes were performed using ICP-MS and co-staining confocal microscopy. ICP-MS experiments were used to analyze the subcellular distribution of the complexes in HeLa cells. HeLa cells were incubated with **Ir1-5** (2 μ M) at 37 °C for 30 min (1×10^6 cells) in normoxia and hypoxia. The cells were washed twice with 1 mL PBS, digested with trypsin and counted. All the cells were equally divided into two parts and processed with Nucleus Extraction Kit and Cytoplasmic and Mitochondrial Protein Extraction Kit by the manufacturer's protocols, respectively. The cells were digested by 60% HNO₃ at room temperature for at least 24 h. The standards for calibration were freshly prepared by Ir standard stock solution (1000 μ g/mL) with 2% HNO₃ in Milli-Q H₂O, concentration in extratants was determined by ICP-MS. (Thermo Elemental, USA). For co-localization confocal microscopy. HeLa cells were seeded onto 35 mm confocal dishes with a density of 5×10^4 cells/mL (2 mL) for 24 h in normoxic conditions, then transfer the cell to the hypoxic conditions 12 h. Before incubation with 5 μ M MitoTracker Green for 30 min, the cells were incubation with 2 μ M **Ir1-5** for 30 min at 37 °C, respectively. Prior to Confocal images were aquired the cells were washed twice with 1 mL PBS.

Live/dead viability/cytotoxicity assay in the MCTSs

The live/dead assay for the MCTSs was performed using the live/dead viability/cytotoxicity kit for mammalian cells (Life Technologies). Live cells were distinguished by the existence of ubiquitous intracellular esterase activity, which is determined by the enzymatic conversion of the virtually nonfluorescent. cell-permeable calcein AM to the intensely fluorescent calcein ($\lambda_{\text{ex}} = 495$ nm, $\lambda_{\text{em}} = 515$ nm). EthD-1 is excluded by the intact plasma membrane of live cells but enters the cells with a damaged membrane and undergoes a 40-fold enhancement of fluorescence when binding to nucleic acids, producing a bright red fluorescence in dead cells ($\lambda_{\text{ex}} = 495$ nm, $\lambda_{\text{em}} = 635$ nm). After treatment with **Ir1-5**, MCTSs were incubated with a solution

(10 mL) of calcein AM (2 μ M) and EthD-1 (4 μ M) for 60 min in the dark and imaged directly using an inverted fluorescence microscope (Zeiss Axio Observer D1, Germany).

Acridine orange/ethidium bromide (AO/EB) staining

HeLa cells were seeded into 12-well microtiter plates at a density of 1×10^4 cells (2 mL) per well and cultured in normoxic conditions for 24 h, before transfer of the cells to hypoxic conditions for 12 h. The medium was changed and the cells treated with complexes **Ir1-5** (2 μ M) for 24 h in hypoxia. After this the cell culture medium was removed, and the cells were stained with 1 mL AO/EB solution (100 mg mL⁻¹ AO, 100 mg mL⁻¹ EB, 10 min) diluted in PBS, using an inverted fluorescence microscope for imaging analysis. (Zeiss Axio Observer D1, Germany).

Induction of mitochondrial dysfunction

Mitochondrial transmembrane potential was assessed by measurement with JC-1. HeLa cells were cultured onto 35 mm confocal dishes for 24 h in normoxic conditions (2 mL, 5×10^4 cells/mL single cell), then transferred to hypoxic conditions for 12 h. Subsequent treatment with complexes **Ir1-5** (2 μ M) for 6 h and CCCP 10 μ M for 5 min in hypoxia, was followed by staining with JC-1 (5 μ g/mL, 15 min). The cells were washed twice with 1 mL PBS and changes in the mitochondrial membrane potential were measured by confocal laser scanning microscopy.

Caspase-3 activation detection

Caspase-3 activity was measured using Caspase-Glo 3/7 assay kit (Promega, USA), HeLa cells were seeded in white 96-well plates at a density of 1×10^4 cells 24 h (90 μ L), and the negative control was incubated with pure culture medium. Cisplatin (20 μ M) as the positive control and complexes **Ir1-5** (2 μ M) as the experimental group were incubated for 12 h at 37 °C in hypoxic conditions. Each column represents the average

of triplicates from three independent experiments. 100 μ L of Caspase-Glo 3/7 reagent was added to each well, and incubated for 1 h at room temperature in the dark to give a final volume of 200 μ L. The luminescence intensity was measured by a multifunction microplate reader (infinite M200 PRO, TECAN).

Western blot analysis:

HeLa cells were seeded into 100 mm tissue culture dishes, then incubated under hypoxia for 24 h. **Ir1-5** (2 μ M) was added for another 24 h under hypoxia. The cells were washed with precool PBS and lysed in the buffer of radio immune precipitation assay buffer (RIPA) with a protease inhibitor cocktail (Blue Skies) for 30 min on ice. The lysates were centrifuged at 15000 rpm for 15 min at 4 $^{\circ}$ C, and the protein concentrations were quantified by a BCA protein assay reagent kit (Blue Skies). The proteins were separated on precast NuPAGE 4% to 12% polyacrylamide gradient Bis-Tris gels under denaturing conditions, transferred to PVDF membranes (Invitrogen), and subjected to Western blot analysis. Rabbit monoclonal NOX4 and GAPDH (Blue Skies) antibodies were diluted in PBS containing nonfat powdered milk (5%) and Tween-20 (0.1%) and then incubated with the membrane overnight at 4 $^{\circ}$ C. Horseradish peroxidase conjugated secondary antibodies (Blue Skies) were used. The signal of the protein was detected using an ECL prime Western blot detection reagent (Amersham Inc., USA).

Real-time monitoring of hypoxic cell assay

HeLa cells were cultured onto 35 mm confocal dishes for 24 h in normoxic conditions (2 mL, 5×10^4 cells/mL single cell, 5% CO₂, 20 % O₂, 10% FBS, 1% penicillin-streptomycin at 37 $^{\circ}$ C), and then the cells were cultured under hypoxic conditions 12 h (1 % O₂) and treated with **Ir2** (2 μ M). The cell morphology was captured by a differential internal confocal microscope under hypoxic conditions.

Supporting Figures

2019215-19215114307#416 RT: 1.21 AV: 1 SB: 161 0.63-1.10 NL: 5.85E6
T: ITMS + cESI Full ms [50.00- 1250.00]

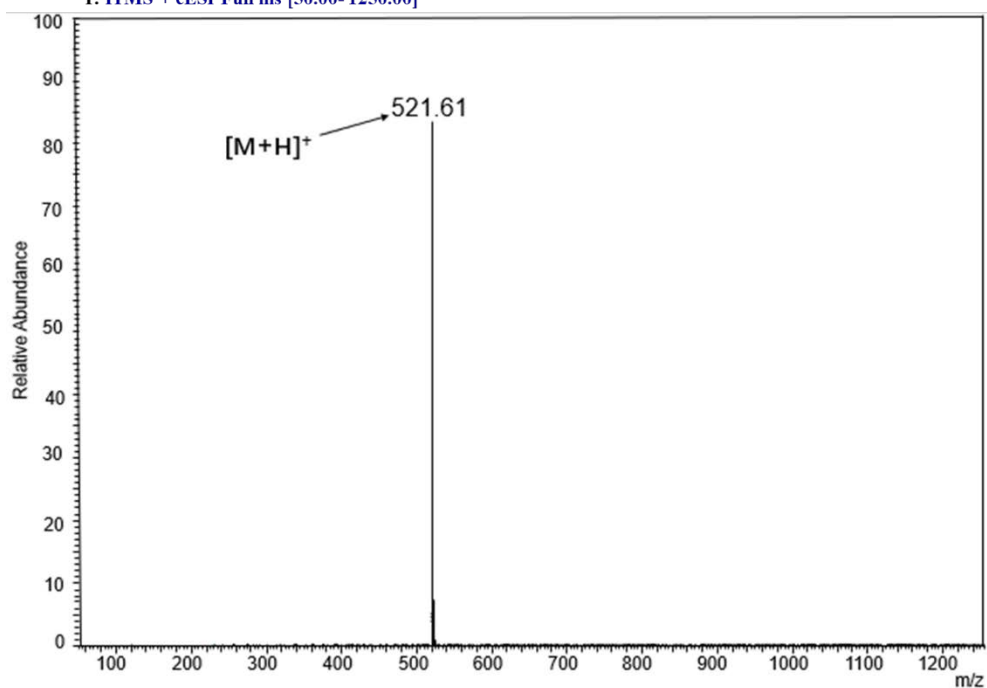


Figure S1 ESI-MS spectrum of L3.

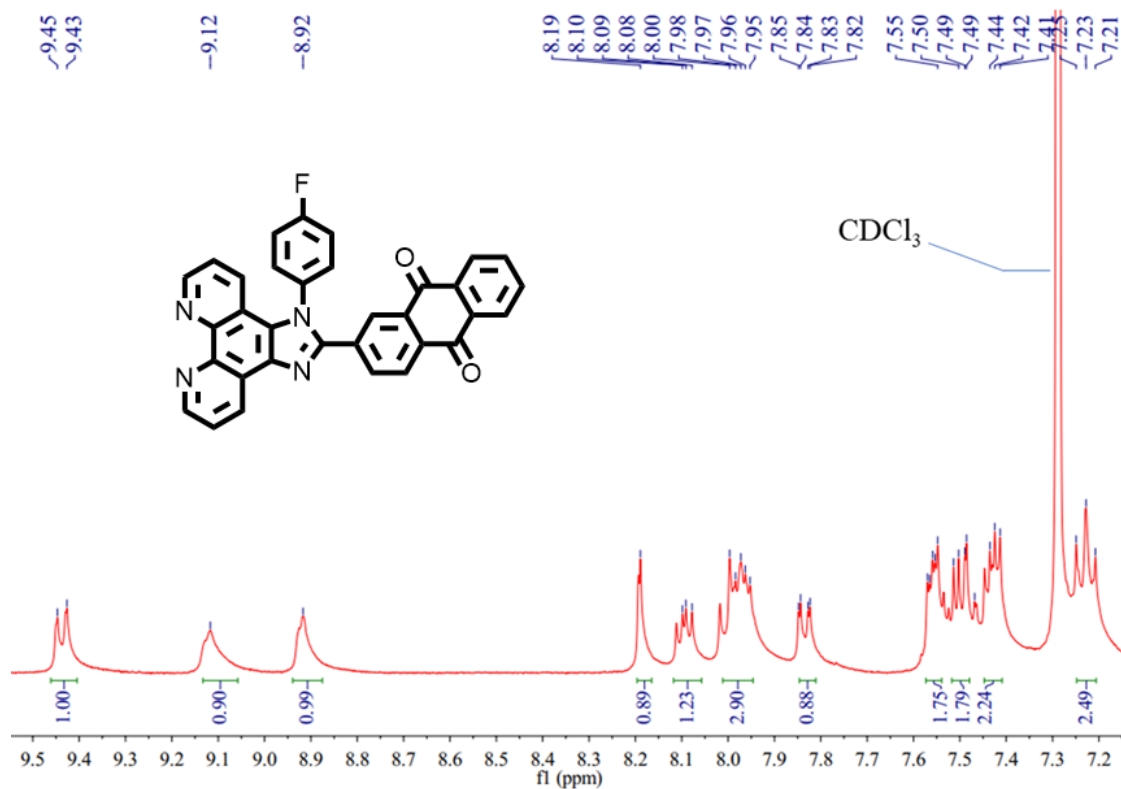


Figure S2 ^1H NMR spectrum of L3.

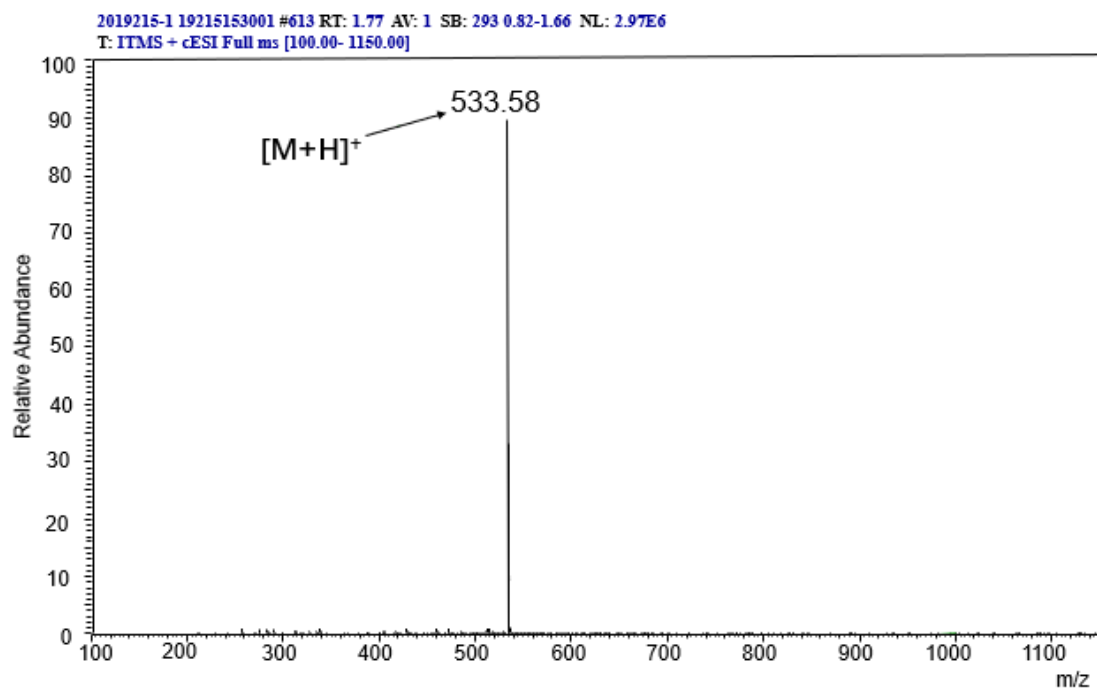


Figure S3 ESI-MS spectrum of L4.

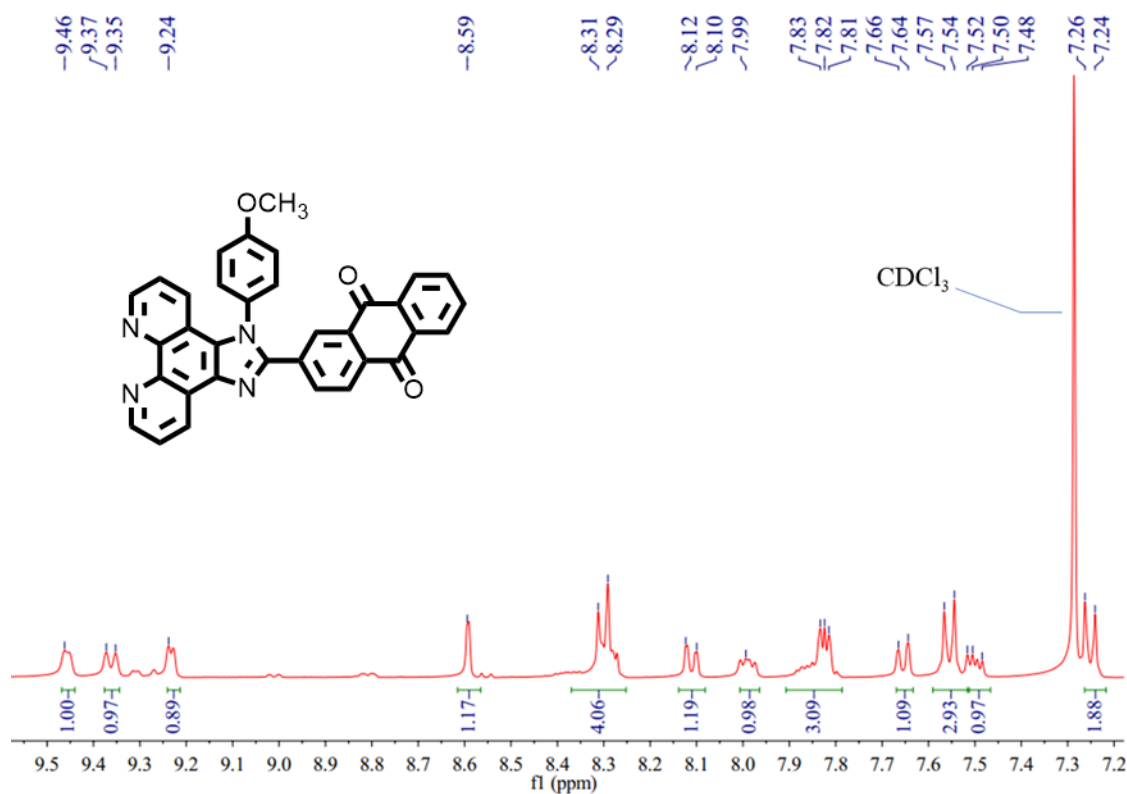


Figure S4 ^1H NMR spectrum of L4.

2019215-1 19215114307 #979 RT: 2.85 AV: 1 SB: 222 2.06-2.71 NL: 5.00E6
T: ITMS + cESI Full ms [50.00- 1050.00]

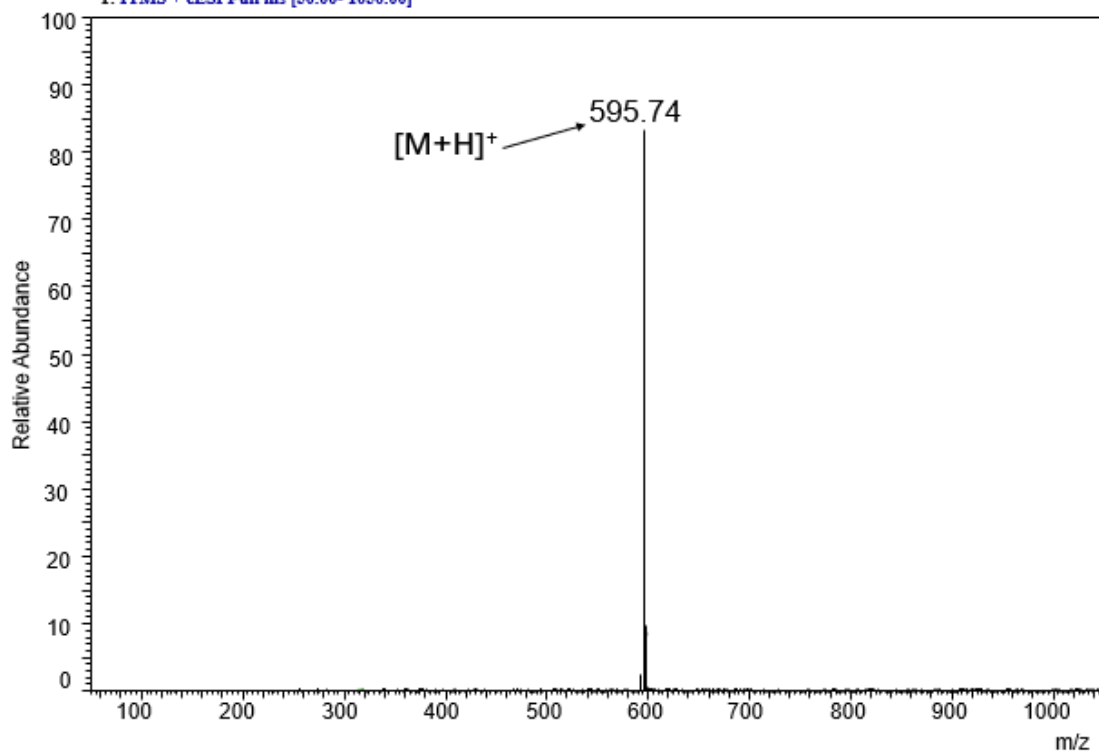


Figure S5 ESI-MS spectrum of L5.

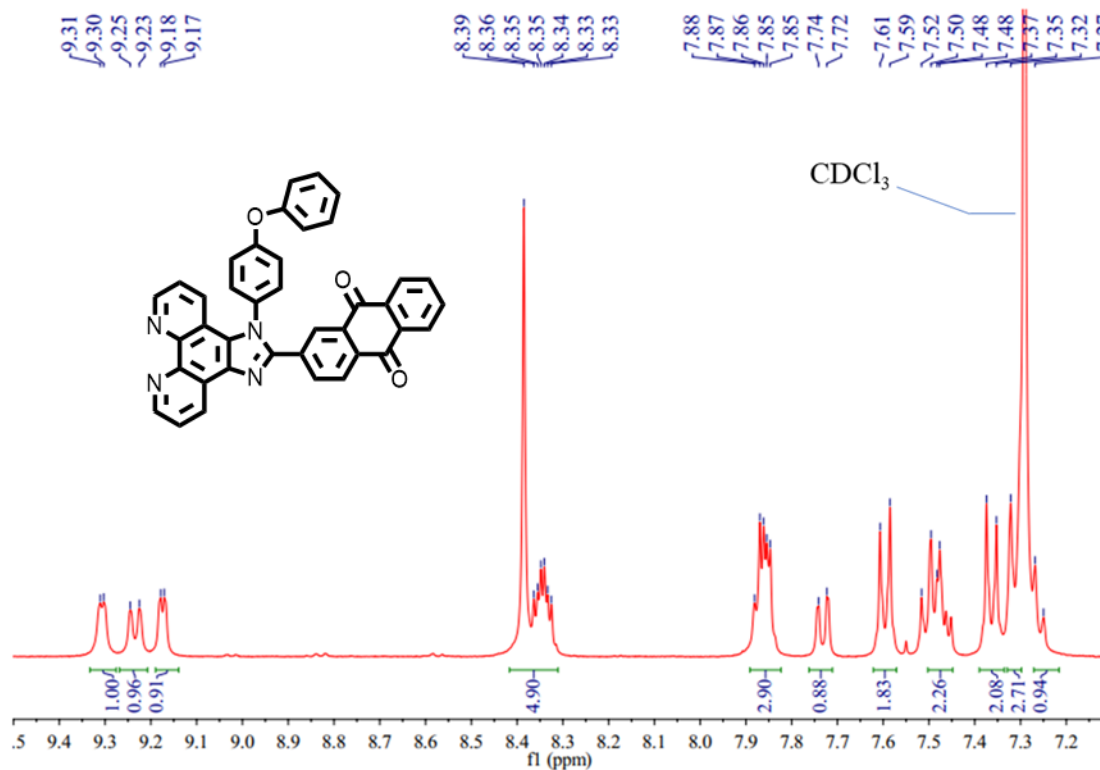


Figure S6 ^1H NMR spectrum of L5.

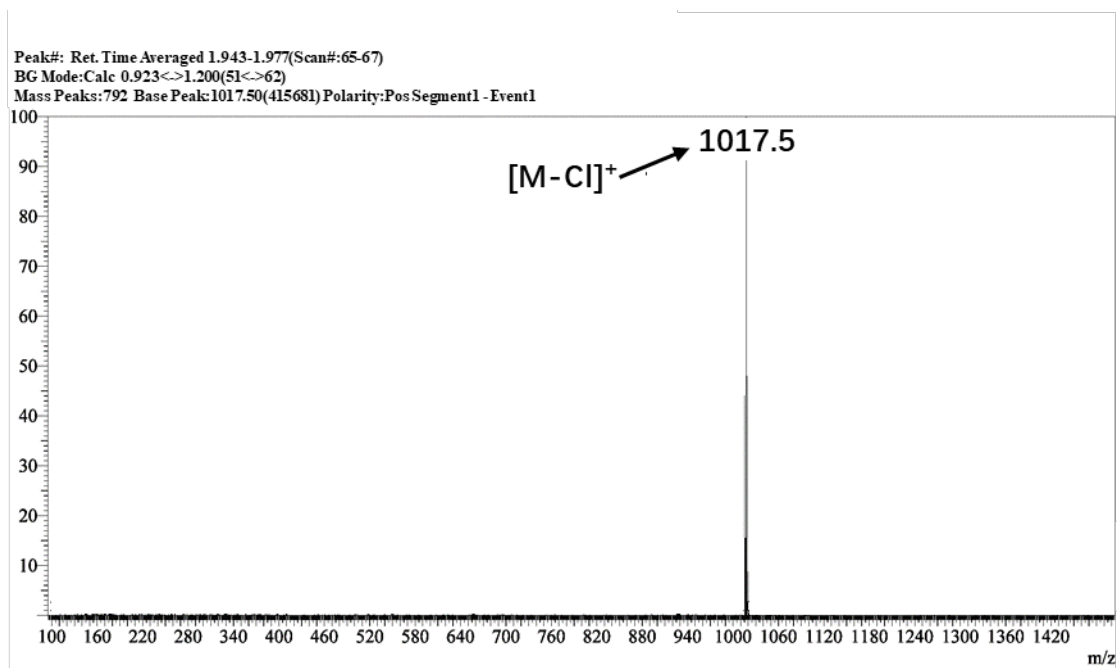


Figure S7 ESI-MS spectrum of Ir1.

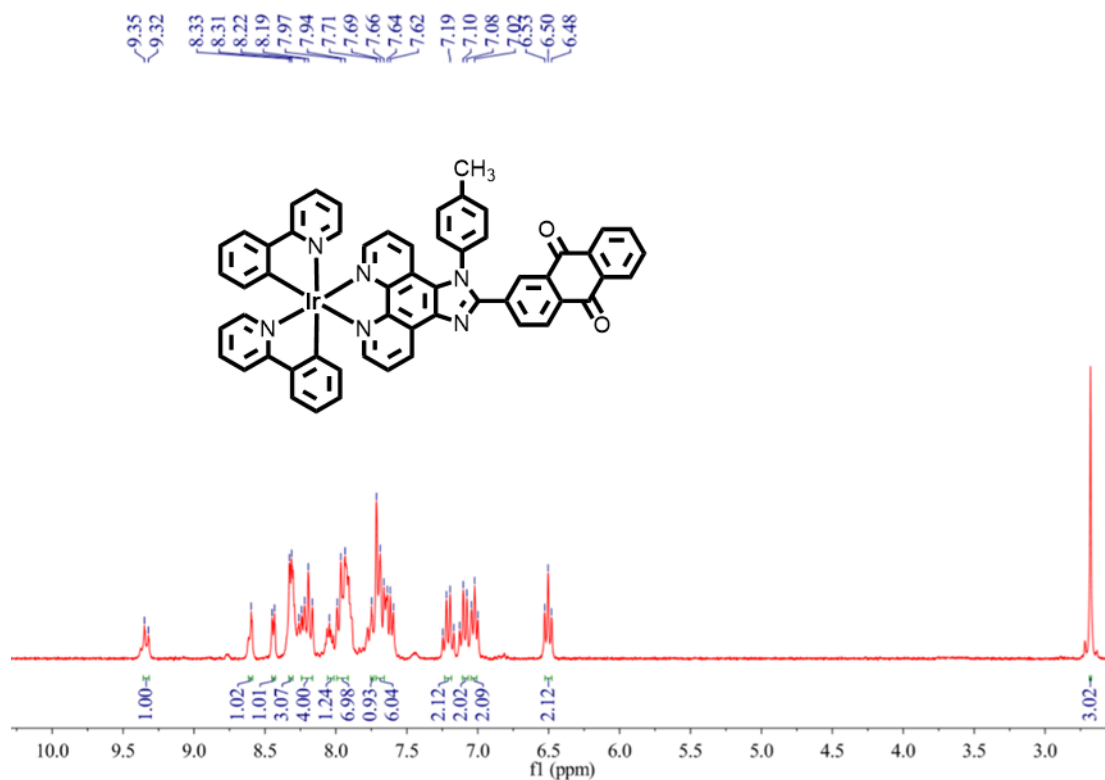


Figure S8 ^1H NMR spectrum of Ir1.

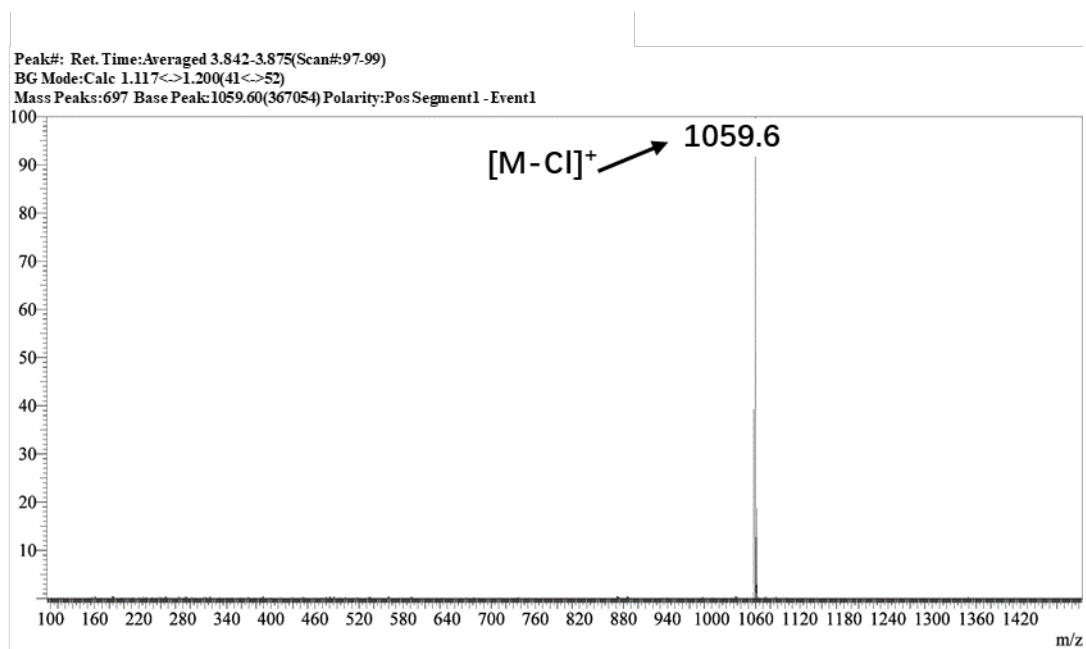


Figure S9 ESI-MS spectrum of Ir2.

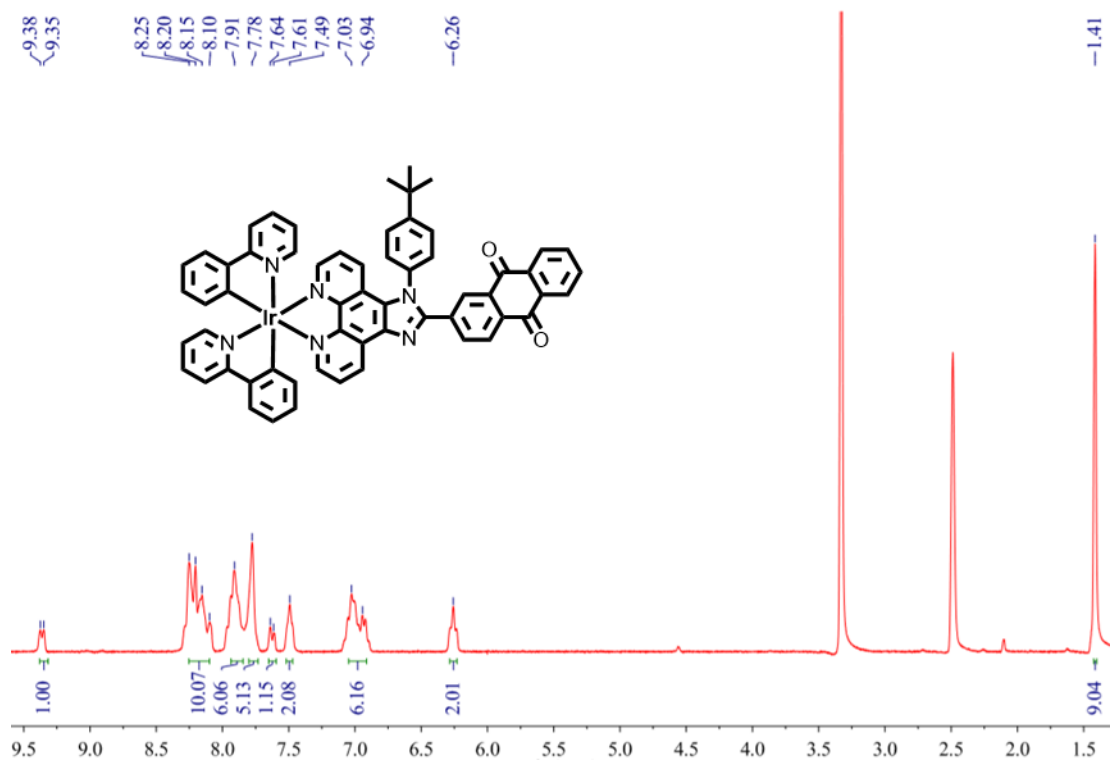


Figure S10 ¹H NMR spectrum of Ir2

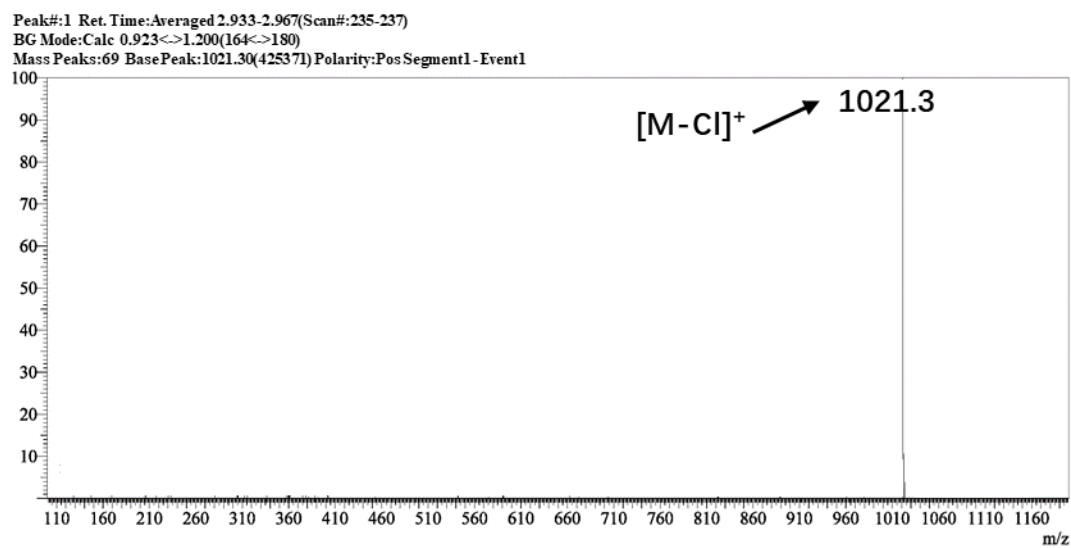


Figure S11 ESI-MS spectrum of **Ir3**.

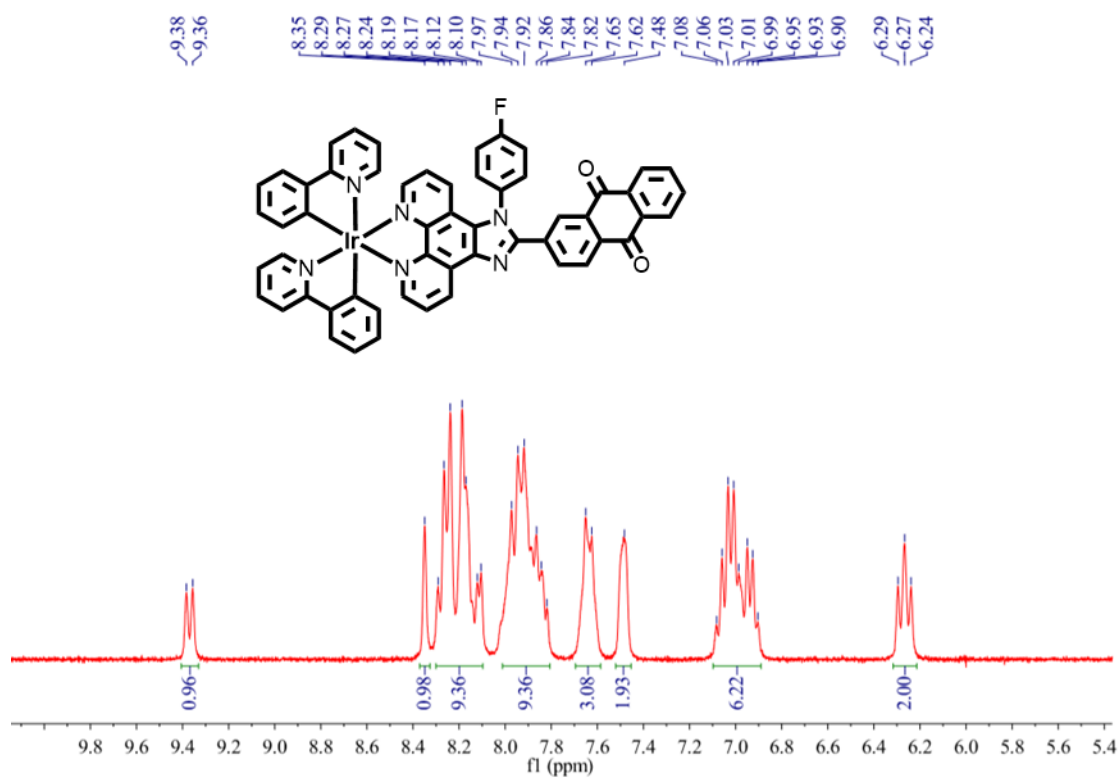


Figure S12 ¹H NMR spectrum of **Ir3**.

Peak#:1 Ret. Time:Averaged 6.800-6.833(Scan#:315-317)
BG Mode:Calc 1.123<->1.300(164<->180)
Mass Peaks:79 BasePeak:1033.20(20245) Polarity:Pos Segment1 - Event1

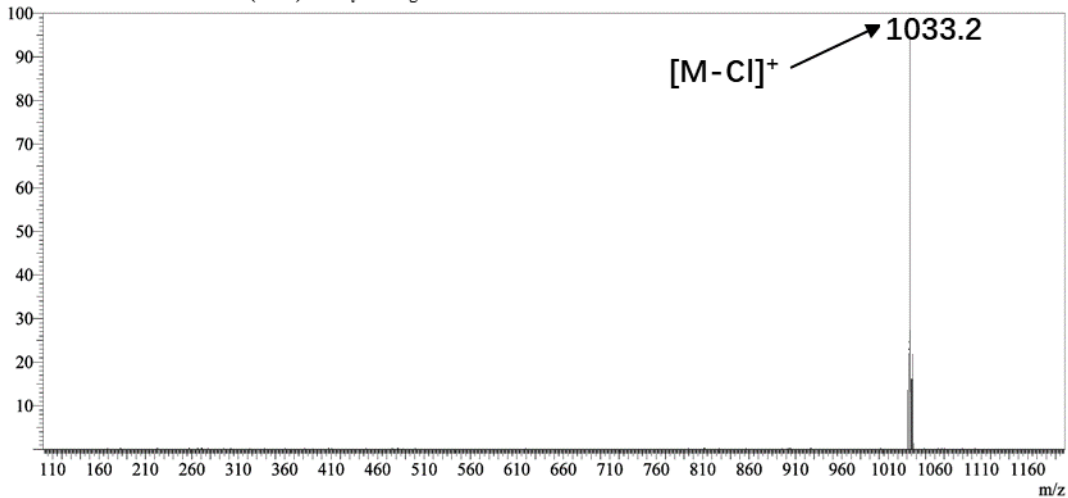


Figure S13 ESI-MS spectrum of Ir4.

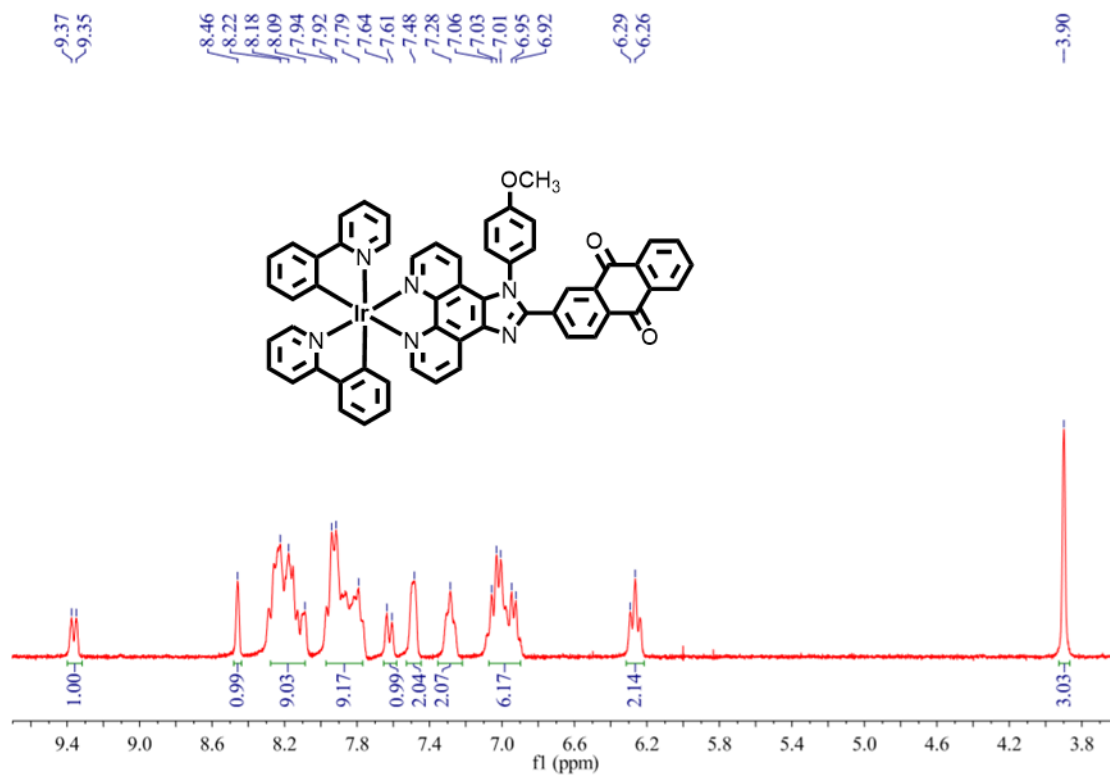


Figure S14 ¹H NMR spectrum of Ir4.

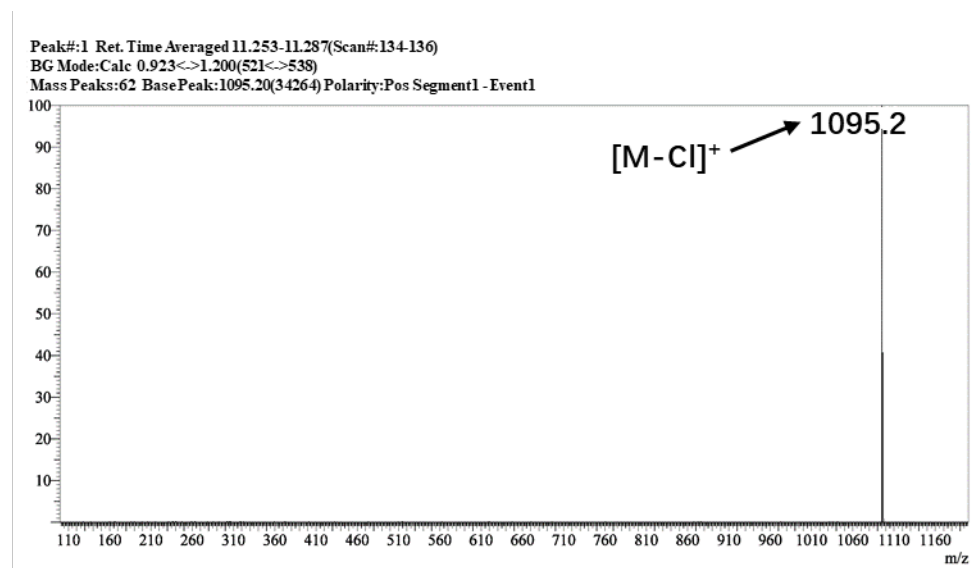


Figure S15 ESI-MS spectrum of **Ir5**.

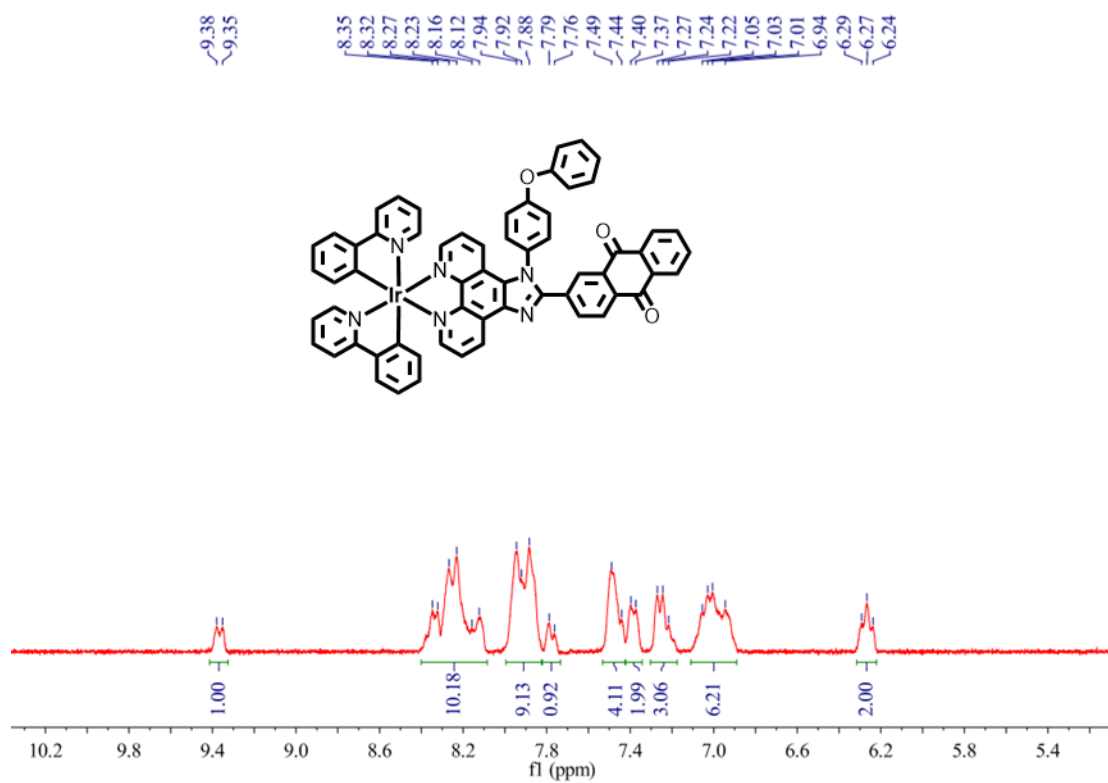


Figure S16 ^1H NMR spectrum of **Ir5**.

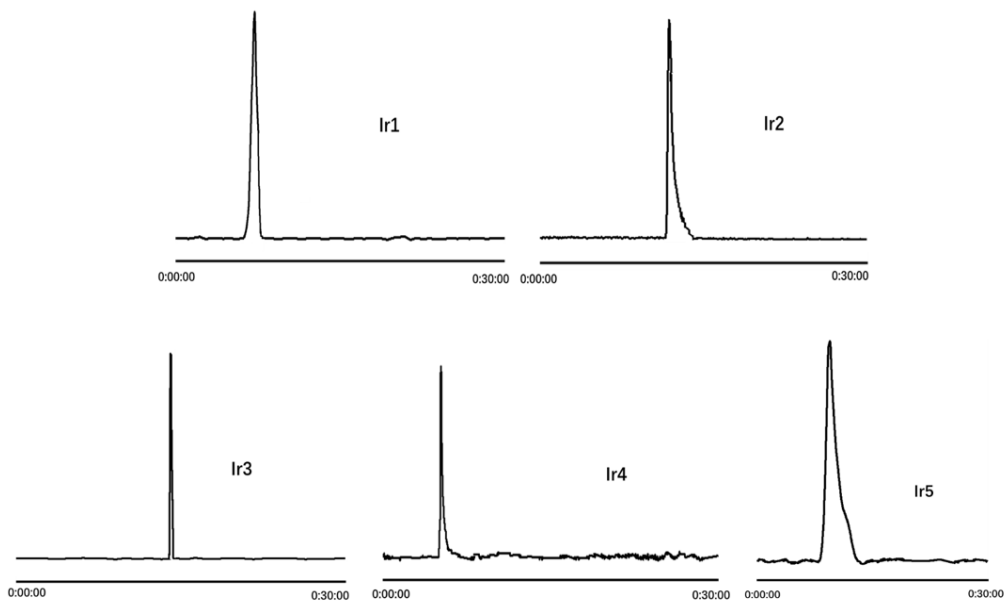


Figure S17 The HPLC spectra of **Ir1-5**.

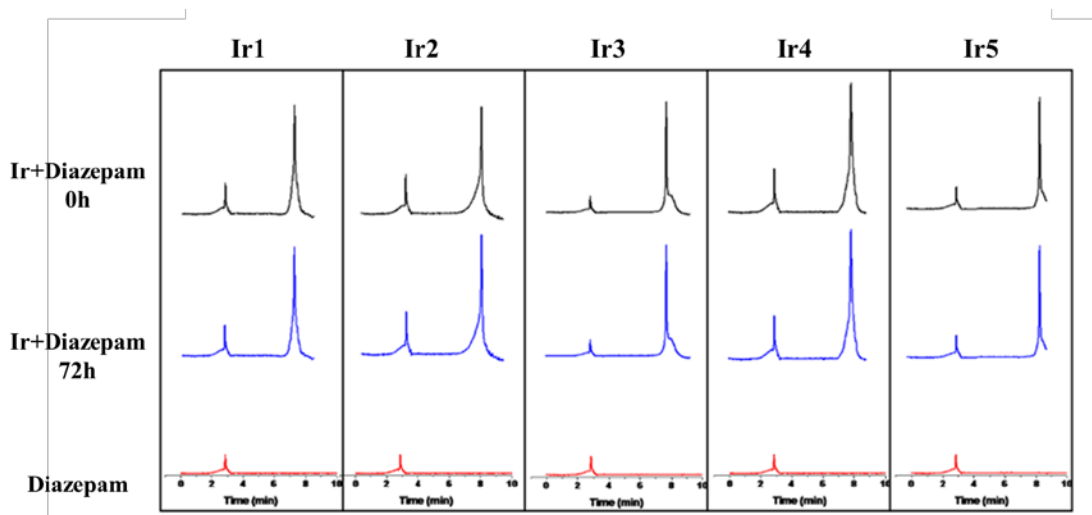


Figure S18 LC-UV trace of plasma incubated with **L1-Ir5** ($10.0 \mu\text{M}$) at $t = 0$ and 72 h (Diazepam was used as internal standard).

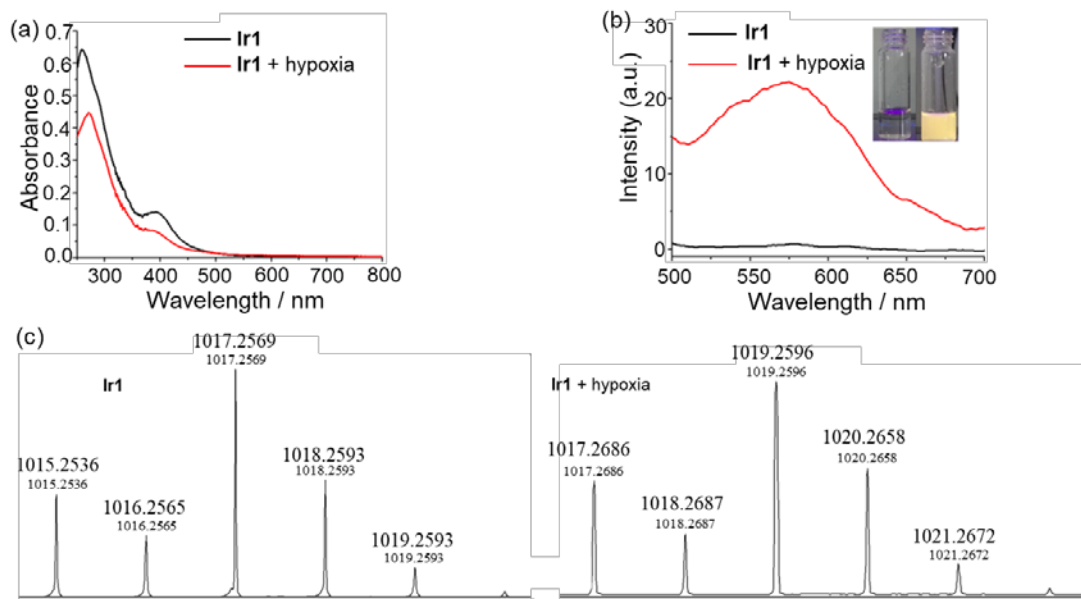


Figure S19 The change of absorption spectra a) and phosphorescence spectra b) of **Ir1** (10 μ M) were compared before and after incubation in hypoxia condition (NADPH: 50 μ M, rat liver microsomes: 0.25 mg/mL and nitrogen atmosphere) for 6 h (λ_{ex} = 400 nm). Insert: photographs of **Ir1** solution under normoxic (left) or hypoxic (right) conditions under excitation of 365 nm brevity desktop UV analysis. c) HRMS spectra of **Ir1** and its reduction products under hypoxia condition.

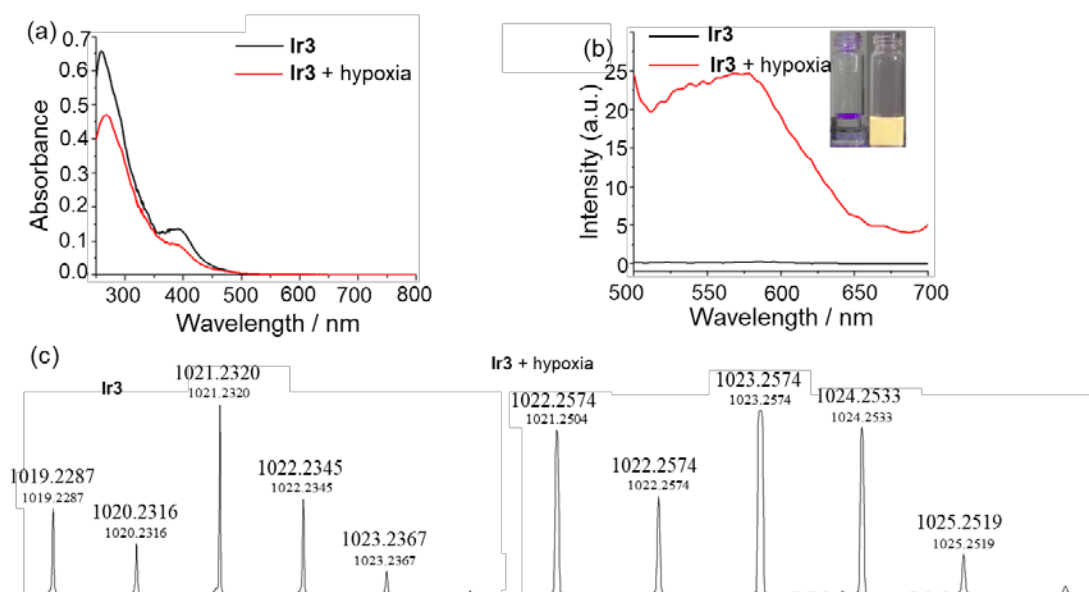


Figure S20 The change of absorption spectra a) and phosphorescence spectra b) of **Ir3** (10 μ M) were compared before and after incubation in hypoxia condition (NADPH: 50 μ M, rat liver microsomes: 0.25 mg/mL and nitrogen atmosphere) for 6 h (λ_{ex} = 400 nm). Insert: photographs of **Ir3** solution under normoxic (left) or hypoxic (right) conditions under excitation of 365 nm brevity desktop UV analysis. c) HRMS spectra of **Ir3** and its reduction products under hypoxia condition.

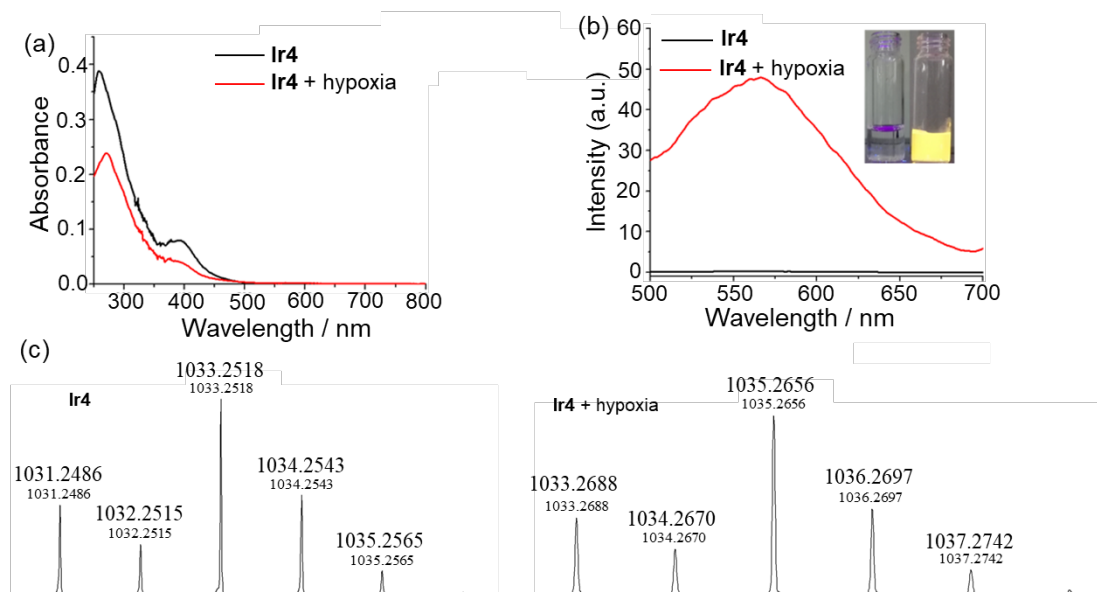


Figure S21 The change of absorption spectra a) and phosphorescence spectra b) of **Ir4** (10 μ M) were compared before and after incubation in hypoxia condition (NADPH: 50 μ M, rat liver microsomes: 0.25 mg/mL and nitrogen atmosphere) for 6 h ($\lambda_{\text{ex}} = 400$ nm). Insert: photographs of **Ir4** solution under normoxic (left) or hypoxic (right) conditions under excitation of 365 nm brevity desktop UV analysis. c) HRMS spectra of **Ir4** and its reduction products under hypoxia condition.

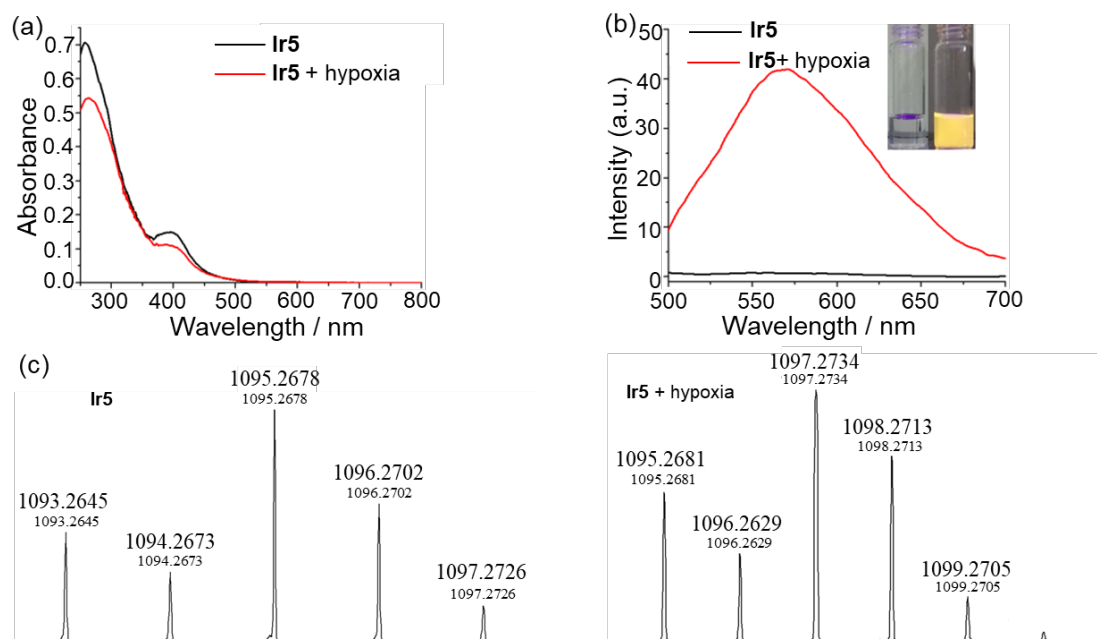


Figure S22 The change of absorption spectra a) and phosphorescence spectra b) of **Ir5** (10 μ M) were compared before and after incubation in hypoxia condition (NADPH: 50 μ M, rat liver microsomes: 0.25 mg/mL and nitrogen atmosphere) for 6 h ($\lambda_{\text{ex}} = 400$ nm). Insert: photographs of **Ir5** solution under normoxic (left) or hypoxic (right) conditions under excitation of 365 nm brevity desktop UV analysis. c) HRMS spectra of **Ir5** and its reduction products under hypoxia condition.

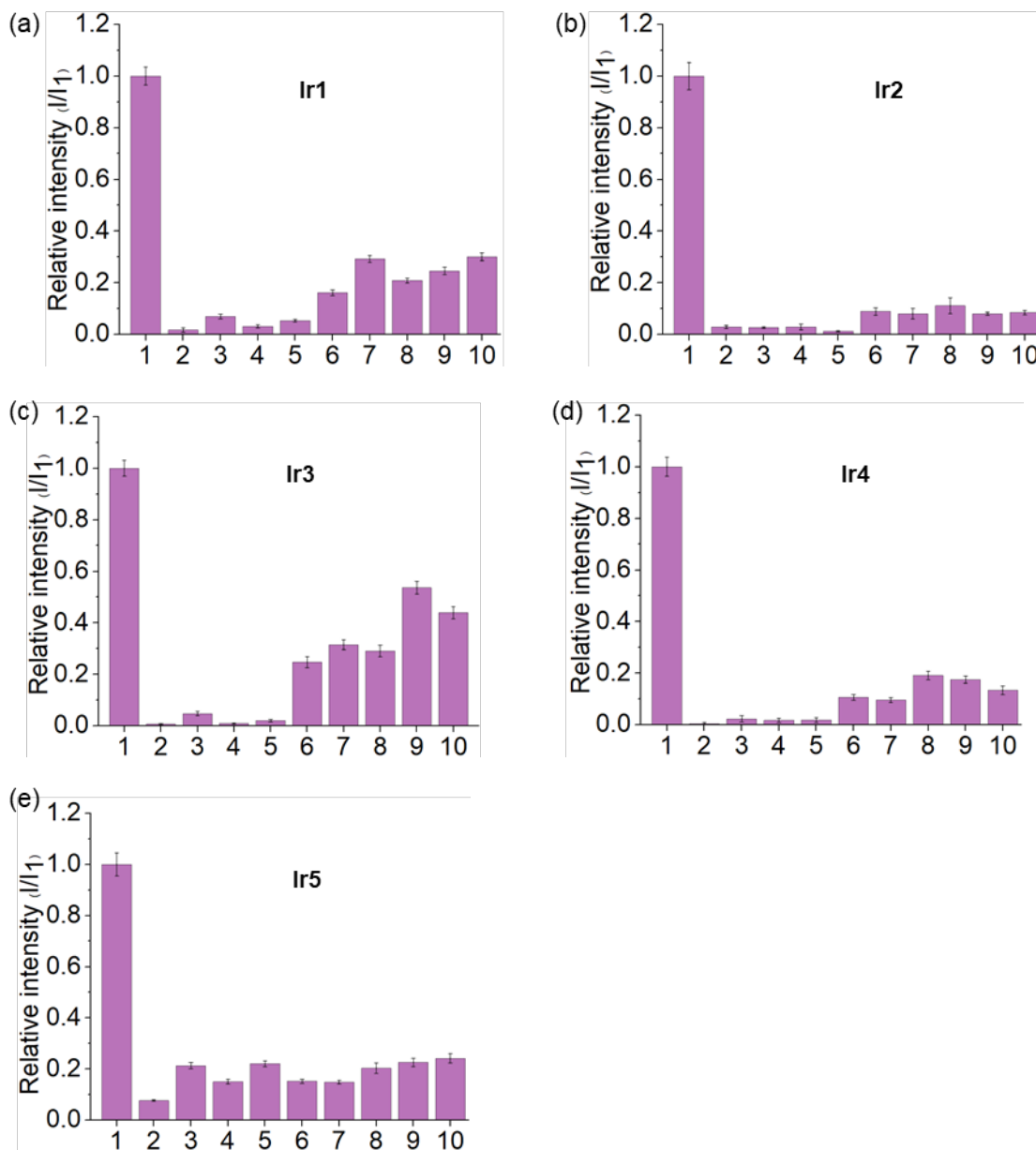


Figure S23 Relative emission intensity of **L1-5** a), b), c), d), e) (10 μ M) under hypoxia upon the addition of NADPH (50 μ M Bar 1) in the presence of different background reducing ions or bio-relative species (500 μ M), potassium phosphate buffer (pH = 7.3) contained rat liver microsomes (0.25 mg/mL). Bar (1) NADPH, (2) Ascorbic Acid, (3) GSH, (4) Met, (5) Cys, (6) S^{2-} , (7) NO_2^- , (8) $S_2O_3^{2-}$, (9) SO_3^{2-} , (10) HSO_3^- . $\lambda_{ex} = 400$ nm, $\lambda_{em} = 570$ nm.

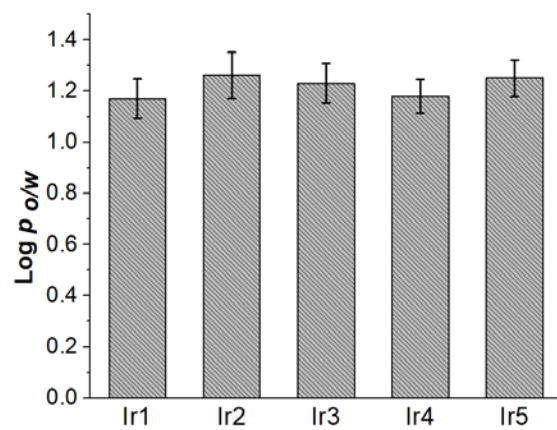


Figure S24 Octanol/water partition coefficients of **Ir1-5**, the error bars denote standard deviation calculated from three replicate trials.

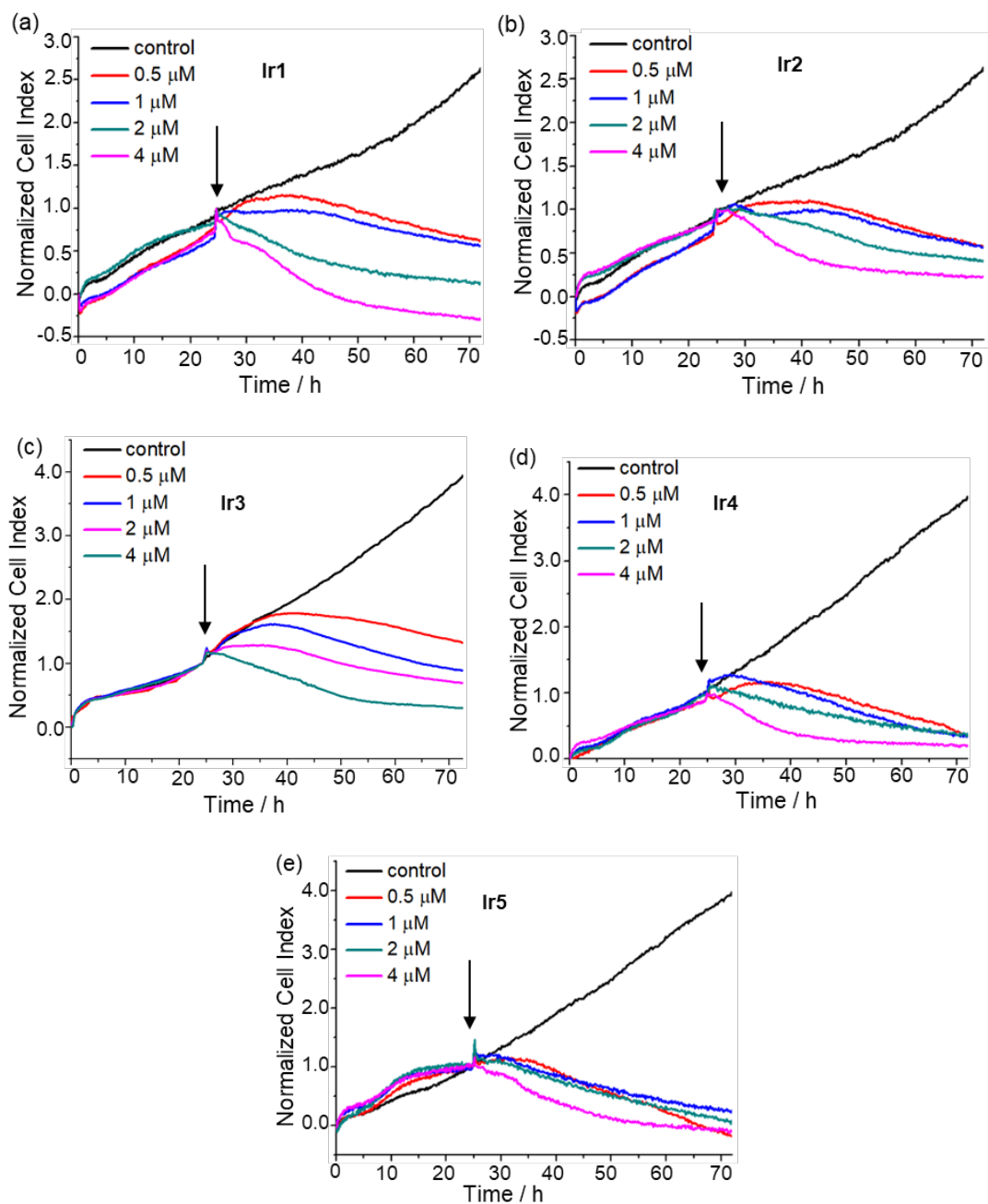


Figure S25 Growth kinetics of HeLa cells for complex **Ir1-5** with different concentrations be monitored by the xCELLigence system in hypoxia. 5000 cells were plated in per well with 16-well plate for the RT-CES cytotoxicity assay. The arrows mean the addition of the Ir(III) complexes.

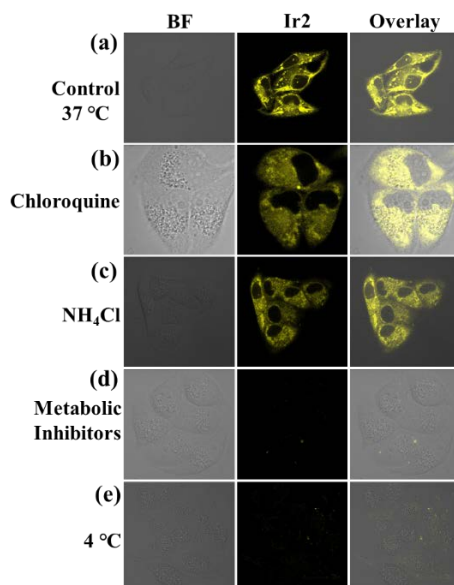


Figure S26 Confocal phosphorescence images of living HeLa cells incubated with 2 μM **Ir2** in PBS under different conditions. (a) The cells were incubated with **Ir2** at 37 °C for 1 h. (b and c) The cells were pretreated with endocytic inhibitors chloroquine (100 μM) and NH_4Cl (50 mM), respectively, and then incubated with **Ir2** at 37 °C for 1 h. (d) The cells were preincubated with 50 mM 2-deoxy-D-glucose and 5 μM oligomycin in PBS for 1 h at 37 °C and then incubated with 2 μM of **Ir2** at 37 °C for 1 h. (e) The cells were incubated with **Ir2** at 4 °C for 1 h.

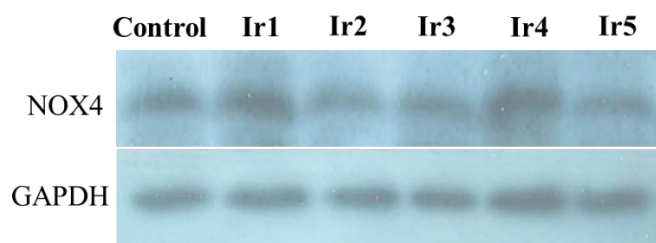


Figure S27 Western blot analysis was performed with NOX4 after treatment with **Ir1-5** hypoxia HeLa cells.

References

- [1] P. Zhang, H. Huang, Y. Chen, J. Wang, L. Ji, H. Chao, *Biomaterials*, 2015, **53**, 522.
- [2] J. Liu, C. Jin, B. Yuan, X. Liu, Y. Chen, L. Ji, H. Chao, *Chem. Commun.*, 2017, **53**, 2052.